SAND2015-1502C

Analysis of Laser Weld Induced Residual Stress in a Hermetic Glass-to-Metal Seal

Ryan D. Jamison[a], Pierrette H. Gorman[a], Jeffrey Rodelas[a], Danny O. MacCallum[a], Matthew Neidigk[a], J. Franklin Dempsey[a]

[a]Sandia National Laboratories[1], PO Box 5800, MS 0346, Albuquerque, New Mexico 87185-0346, USA

ABSTRACT
Laser welding of glass-to-metal electrical connectors is a common manufacturing method for creating a hermetically sealed device. The materials in these connectors, in particular the organic glass, are sensitive to thermal induced residual stress and localized heating. An analytical laser weld model is developed that provides simulation and analysis of both thermal and mechanical effects of the welding process. Experimental studies were conducted to measure the temperature at various locations on the connector. The laser weld is modeled using both surface and volumetric heating directed along the weld path to capture the thermal and mechanical response. The weld region is modeled using an elastic-plastic weld material model, which allows for compliance before welding and stiffening after the weld cools. Results from a finite element model of the glass-to-metal seal are presented and compared with experimental results. The residual compressive stress in the glass is reduced due to the welding process and hermeticity is maintained.

KEYWORDS: Laser weld, residual stress, hermetic seal, FEA, thermomechanical

1 Introduction

Glass-to-metal hermetic seals are found in many engineering applications, such as semiconductor electronics, thermostats, optical devices, switches, and electrical connectors. The hermetic seal is traditionally created using one of two methods [1]. First, "matched seals" are seals in which the glass and metal packaging have similar coefficients of thermal expansion (CTE) and rely on chemical bonds between the glass and metal oxide to provide a seal. Second, compression seals, or "mismatched seals", are designed such that the metal surround will shrink more rapidly than the glass, putting the glass in compression and creating a seal. Hermetic seals used as electrical connectors typically involve a metallic shell and contact(s) and an organic or inorganic glass. A common approach for designing hermetic connectors is to use a contact material whose CTE matches that of the sealing glass and a shell material that creates compression seal around the glass and contact. Fig. 1 shows an example of a hermetic connector. In the figure, the hermetic connector consists of a metallic shell, sealing glass, and single contact. Because the hermetic seal is created by taking the connector through a glass sealing cycle at temperatures typically greater than 500 °C, residual stresses are commonly present in the sealing glass and need to be carefully characterized to ensure hermeticity.

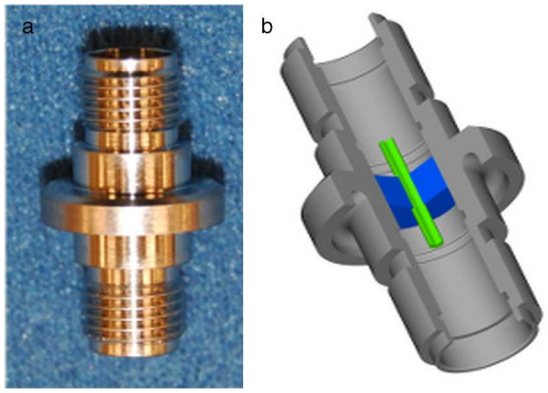

[1] Sandia National Laboratories is a multi-program laboratory managed and operated by Sandia Corporation, a wholly owned subsidiary of Lockheed Martin Corporation, for the U.S. Department of Energy's National Nuclear Security Administration under contract DE-AC04-94AL85000.

Fig. 1 (a) Photo and (b) cross-section of the single contact glass-to-metal seal analyzed in this paper

Hermetic connectors, and seals in general, must be attached to surrounding material using a method that will maintain hermeticity. Methods used to mount hermetic seals include laser, TIG, or MIG welding. One of the most common methods is to laser weld the hermetic seal to the surrounding bulkhead. Laser welding has been studied extensively and many methods have been developed to allow for finite element simulations of the laser welding process [2-6] as well as residual stress in weld members [7-9]. When welding the hermetic connector, large amounts of energy are deposited locally in the connector, which can result in large temperature gradients and high-localized temperatures, causing residual stress. Because of the nature of the "matched" and compression seals found in hermetic connectors, the residual stress in the glass is sensitive to large changes in temperature. Therefore, it is import to understand the residual stress state in the sealing glass after the sealing cycle and welding process.

In this paper, experimental work to characterize the temperature distribution through a hermetic connector and finite element simulations to determine the residual stress in the sealing glass is presented. The experimental setup and results are discussed in Section 2. Finite element simulations of the glass sealing cycle are discussed in Section 3. The finite element simulation of the laser weld with resultant temperature distribution and residual stress is shown in Section 4. Comparisons are made between the experiment and finite element simulations to provide a degree of model validation. Finally, concluding comments are in Section 5.

2 Experimental

2.1 Experimental procedure

Laser welding is a high-energy density process that produces high heating and cooling rates during welding. The purpose of this study is to capture the peak welding temperatures and cooling rates in the hermetic connector during the welding process. The laser system used is an IPG YLS-2000, Ytterbium-Doped Fiber Laser System (1070 nm) with motion control and work station integrated by Mundt & Associates, Inc. Laser power measurements were performed using an Ophir power meter 5000W-ROHS. Tack welding of specimens was performed on the LaserStar Model 1900 spot welder. Temperature data was captured using the iOtech Personal DAQ3000 with a sample rate of 520 Hz. The Type K (Chromel/Alumel) 0.010" diameter thermocouples were attached to the hermetic connector and test plate using a Unitek Model 350 resistance welder. Measurements of thermocouple placement were performed on the Vision Engineering Hawk Elite Mono Dynascope.

Prior to welding the hermetic connector, a series of weld bead on sheet experiments were conducted. These experiments were used to provide insight into the power settings of the laser in association with the materials of interest. The sheets used were type 304L stainless steel. Power levels of 300, 350, 400, 450, and 500 W were considered. Metallography was performed on the 300 W and 400 W to visualize the cross-section of the resulting weld bead. Fig. 2 shows the cross-section of the weld beads for 300 and 400 W.

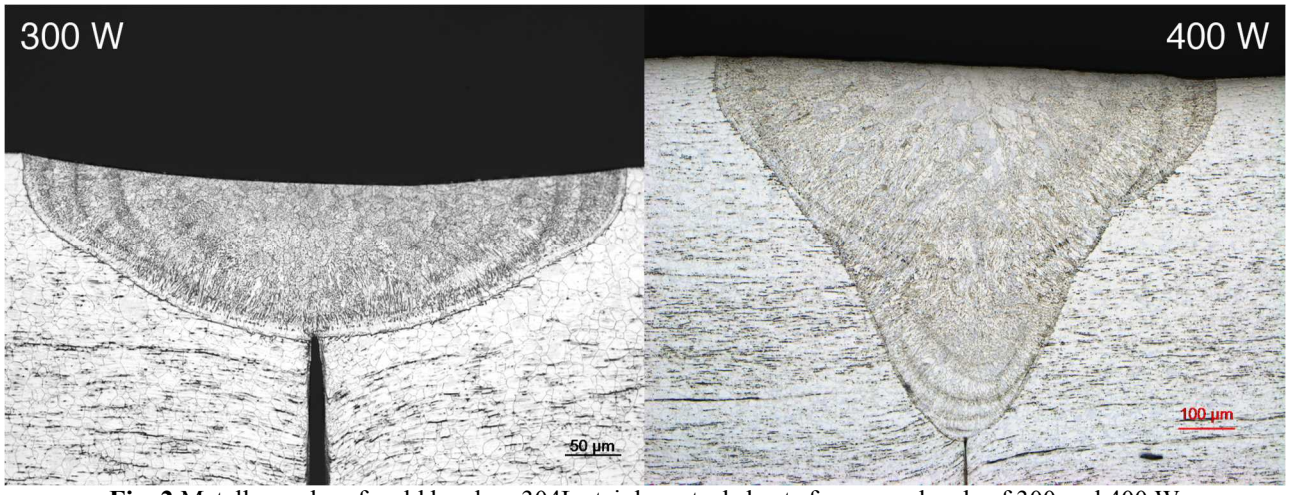

Fig. 2 Metallography of weld bead on 304L stainless steel sheets for power levels of 300 and 400 W

The hermetic seal was welded to a 0.5" thick 304L stainless steel test plate. A hole was machined in the center of the test plate, with geometric features representing a weld flange. Four thermocouples (channels 0 to 3) were placed at 90° increments on the underside of the connector (opposite the side that is welded). One thermocouple (channel 4) was placed

near the weld joint on the underside of the test plate and another (channel 5) was placed on the topside of the test plate near the weld joint opposite channel 4. The placement of the thermocouples is shown in Fig. 3.

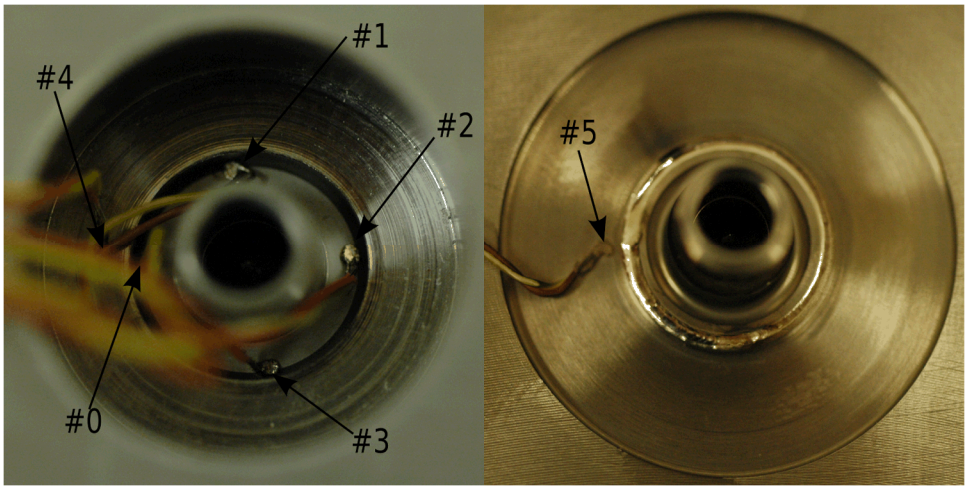

Fig. 3 (a) The underside of the connector showing thermocouples #0 through #4 and (b) the topside of the connector showing thermocouple #5 located on the test plate near the weld joint

The hermetic connector was cleaned with IPA and thermocouples were resistance welded to the 304L sheet. Inert gas shielding (argon) was delivered to the hermetic connector coaxially with the laser beam at a flow rate of 100 cfh. Prior to welding, the connector was tack welded to the test plate at 90° increments around the perimeter of the connector. The sample was welded at 80 in/min travel speed at a nominal power of 338 W. The weld was performed using continuous wave output without modulation. After traveling the full circumference of the connector, the weld was overlapped by 40° at full power and then the power was ramped down to 0 W over an additional 40°. The weld penetration was nominally 0.020" and the weld spot size was approximately 0.011". Two weld passes were made directly on top of each other; the second after the first had cooled to room temperature.

2.2 Experimental results

The temperature at six thermocouple locations was measured during the welding process. The temperature at each thermocouple for both weld passes is shown in Fig. 4. During the first weld pass (image a), the weld transitioned between conduction and keyhole mode welding. As a result, energy transfer efficiency varied along the weld length. The high temperatures in the shell of the hermetic connector are because the virgin weld joint minimizes heat transfer from the connector to the test plate. During the second pass, the peak temperatures are lower due to an increase in allowable heat transfer through the shell and test plate.

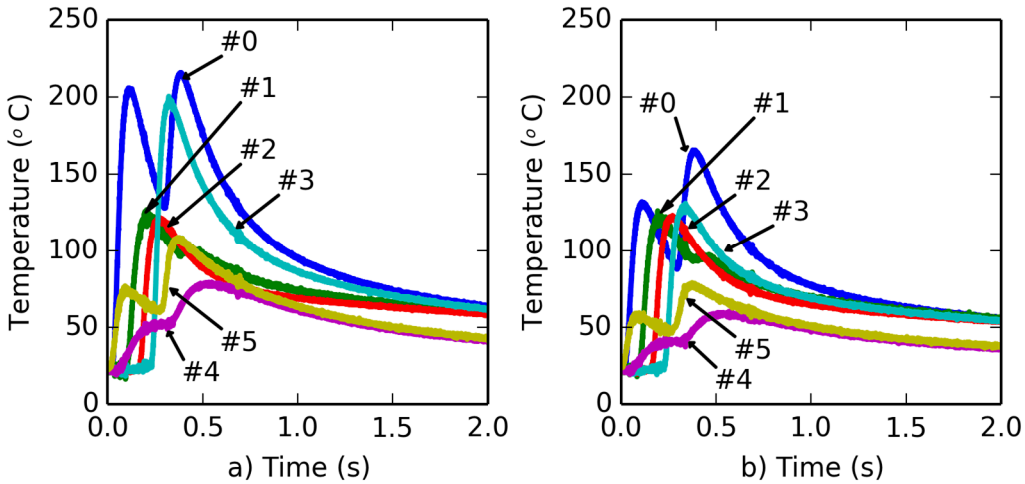

Fig. 4 Experimentally measured temperature at thermocouple locations for (a) first weld pass and (b) second weld pass

3 Finite element model

Though the experimental technique described above is capable of evaluating the temperature in the shell of the hermetic connector during the welding process, it remains difficult to evaluate the temperature of the sealing glass or contact. Also, because of the small size of this particular hermetic connector, it is also difficult to perform any meaningful strain measurements during the welding process. Therefore, finite element modeling is used to analyze the temperature and residual stress in the hermetic connector. The finite element model is composed of two parts – thermal and mechanical. Both codes are built on the SIERRA framework, a massively parallel, finite element code. The thermal modeling of the laser weld is performed in Sierra Thermal/Fluid [10], which specializes in incompressible flow and heat transfer modeling. The residual thermal stresses are calculated using Sierra Solid Mechanics [11], a three-dimensional solid mechanics code capable of modeling nonlinear materials, large deformation, and contact.

3.1 Material models

The materials used in the hermetic connector presented here are those commonly found in many applications. The shell is type 304L Stainless Steel, the contact is Paliney 7, and the sealing glass is Schott S8061. The room temperature thermal and mechanical properties used in the finite simulations are shown in Table 1. Due to a lack of thermal material data at elevated temperatures, room temperature data is used for both Paliney 7 and Schott S8061 for the thermal simulation. Temperature dependent specific heat and thermal conductivity is assumed for the type 304L Stainless Steel.

Three separate solid mechanics material models are used in calculation of the thermal residual stress. The type 304L Stainless Steel is modeled as a thermoelastic-plastic material with temperature dependent Young's modulus, yield stress, and hardening modulus, Paliney 7 is modeled as an elastic-plastic material, and Schott S8061 is modeled as a thermoelastic material with temperature dependent Young's modulus. Though glass is traditionally a viscoelastic material, once the glass cools sufficiently below the glass transition temperature, it begins to behave elastically; therefore, the elastic assumption is valid. The thermal strain profile over the sealing cycle temperature range (-55 °C to 500 °C) for each material is shown in Fig. 5. Lastly, the model assumes the materials are perfectly bonded at all material interfaces.

Table 1 Room temperature thermal and mechanical material properties for the hermetic connector

Material Property	304L SS	Paliney 7	Schott S8061
Density, ρ (kg/m^3)	8,000	11,790	260
Young's modulus, E (GPa)	193	117	68
Poisson's ratio, ν	0.26	0.30	0.21
Yield stress, σ_y (MPa)	241	620	-
Specific Heat, c_p (J/kg-K)	502	240	837
Thermal Conductivity, k (W/m-K)	9.4	71.8	1.05
Melt Temperature, T_m (K)	1,873	-	-

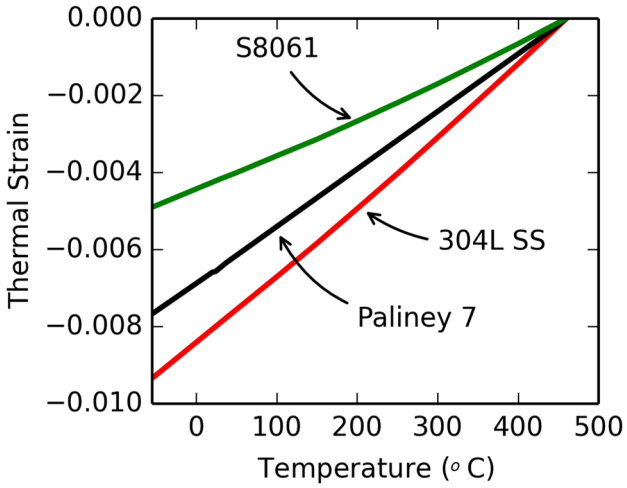

Fig. 5 Linear thermal strain as a function of temperature over sealing cycle temperature range

3.2 Boundary conditions

To model thermal induced residual stresses in a hermetic connector requires both thermal and mechanical simulations. The laser weld modeling capability was developed to evaluate the performance of hermetic connectors and other glass-to-metal

seals subject to laser weld heating. In both simulations, the welded joint is modeled as a thin layer of elements that connect the hermetic shell to the surrounding bulkhead. The solid mechanics material model is assumed elastic-plastic. This assumption allows for simplicity in creating the finite element model while not decreasing the effectiveness of the overall simulation.

In the thermal simulation, the heat transfer in the hermetic connector is modeled assuming Fourier's law heat conduction, surface convection, and black body radiation. The laser weld itself is modeled using both surface and volumetric flux boundary conditions. The surface flux is assumed circular in shape and applies a flux normal to the surface of the weld joint. The radius of the surface flux is assumed to be the spot size of the laser. The volumetric flux is assumed cylindrical in shape and applies a flux to any nodes found within the cylinder. The depth of the volumetric flux is modeled as the nominal penetration depth of the weld and the radius is the same as the spot size. Both surface and volumetric fluxes move in unison in a prescribed path to simulate the welding process. The magnitude of the flux is equal to the measured laser power. To account for losses through the system, both the surface and volumetric flux magnitudes can be scaled independently. The combination of both a surface and volumetric flux is capable of approximating the keyhole formation of a laser weld. For simplicity sake, the material directly affected by the surface and volumetric flux (i.e. the thin weld strip) is assumed to be the same as the bulk material.

The residual stress calculation in the hermetic connector is composed of two simulation steps. The first step consists of isothermal cooling of the entire hermetic connector from 460 °C to room temperature. The model is assumed to be stress free at 460 °C. This step generates the compression on the sealing glass that results in a compression seal. Residual stress is also present in the sealing glass at this stage. The second step consists of applying the resulting temperature field from the thermal simulation. The temperature field from the thermal laser weld simulation is passed to the solid mechanics code as a temperature boundary condition to calculate the thermal residual stress. Prior to heating the weld joint is compliant. Upon heating to melt temperature and subsequent cooling, the material stiffens, producing weld distortion at the weld joint. The weld distortion, thermal expansion of the surrounding material, and the sealing cycle residual stress allows for understanding the complete stress state of the hermetic connector.

3.3 Sealing cycle

Isothermally cooling the hermetic connector from 460 °C to room temperature produces residual stress in the shell, contact, and sealing glass. The residual stress is caused by the mismatched CTE in the sealing glass, contact, and shell. Traditionally for a hermetic connector, it is desired to minimize the maximum principal stress (SMAX) in the sealing glass and prevent (or minimize) plastic strain in the contact and shell. Fig. 6 shows the deformed state of the hermetic connector (magnified 50x) and the maximum residual stress in the sealing glass post sealing cycle. The shell and contact have a greater CTE than the sealing glass, compressing the seal in both the radial and axial directions.

The maximum principal stress in the glass post sealing cycle is very low. Both "matched" and compression seals require that the sealing glass remain in a compressive state. Tensile stress in the sealing glass can lead to glass fracture and loss of hermeticity. For this particular connector, there is very little tensile stress in the sealing glass post sealing cycle. The ring of tensile principal stress that forms (Fig. 6b) is dominated by an axial stress component; therefore, there is little concern of loss of hermeticity in the connector.

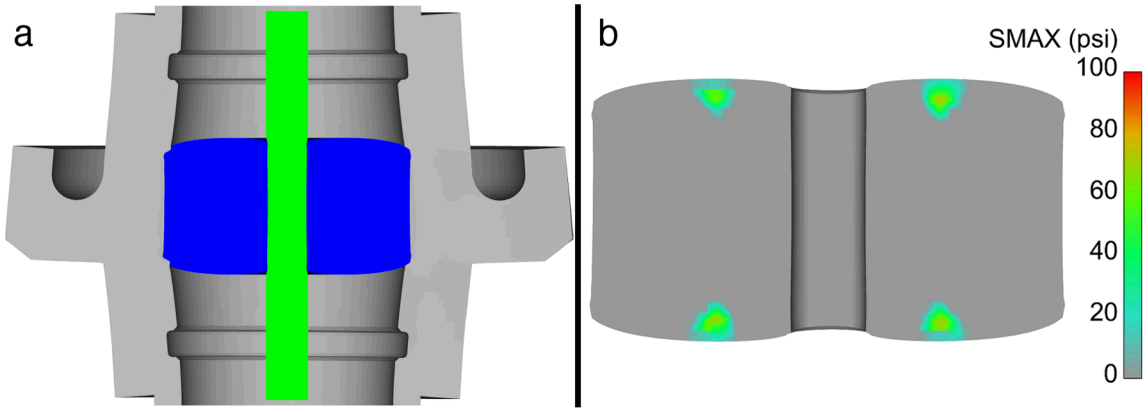

Fig. 6 Hermetic connector post sealing cycle (a) deformation magnified 50x and (b) maximum principal stress in sealing glass in a deformed state (50x magnification)

3.4 Laser weld

The experimental outlined above was able to capture the temperature on the surface of the shell at various locations. This data was used to calibrate the finite element thermal model inputs. The finite element model provides insight into the temperature and stress throughout the sealing glass and contact. The maximum temperature anywhere in the sealing glass and contact is shown in Fig. 7. The peak temperature in the sealing glass reaches is 80 °C and in the contact is 55 °C. The peak temperature in the contact occurs at the axial center of the contact near the contact-glass interface. Furthermore, the peak temperature in both the sealing glass and contact occur after the weld has completed.

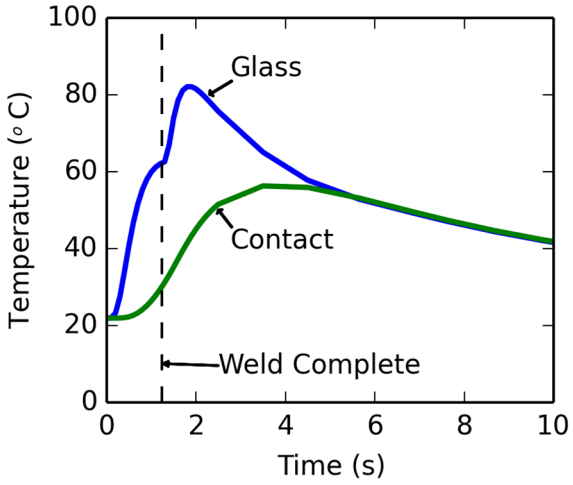

Fig. 7 The maximum temperature anywhere in the sealing glass and contact during the laser weld and post-weld cool down

The temperature distribution throughout the glass is shown in Fig. 8. The temperature is shown at the time corresponding to the peak temperature anywhere in the glass (see Fig. 7). The temperature in the glass is not uniformly distributed and there is a large portion of the glass at or near the peak temperature. The peak temperature occurs near the location of the Ch. 0 thermocouple, which corresponds to the overlap portion of the weld. The resulting thermal gradient is 40 °C. The peak temperature in the glass is sufficiently below the glass transition temperature to avoid any mechanical transition effects. The asymmetric temperature distribution does result in an asymmetric stress distribution.

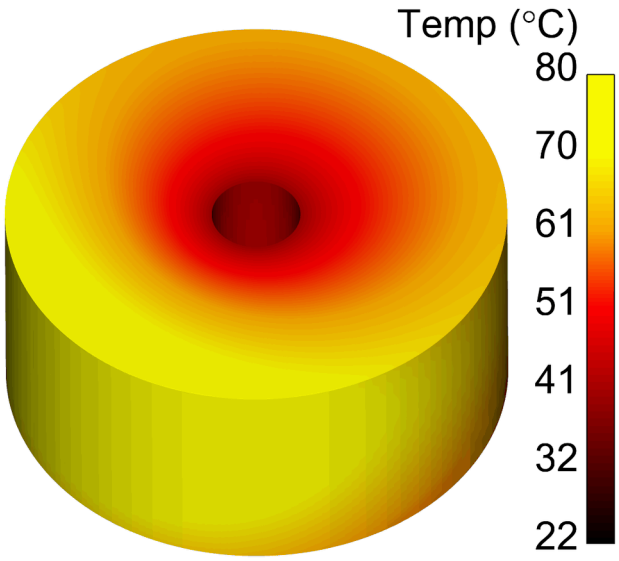

Fig. 8 Temperature distribution in the sealing glass caused by the laser weld at the time corresponding to the peak temperature in the glass

The increase in temperature and asymmetric distribution thereof can lead to an increase in residual stress in the sealing glass. Furthermore, the welding process can affect the radial compression of the sealing glass. Figure 9 shows the post-weld

residual maximum principal stress in the sealing glass as well as the radial compression at the shell-glass and contact-glass interface. The maximum principal stress is shown at the time corresponding to the peak stress during the welding process. There is an insignificant change in residual stress during the welding process. Though the change in maximum principal stress is small, the radial compression decreases by nearly 10 ksi at both the contact and shell interfaces (Fig. 9b). The solid lines show the radial compression prior to welding and the dashed lines show the radial compression post welding. The laser weld appears to cause the shell to contract at the weld location, effectively decreasing the compression imposed on the sealing glass and contact.

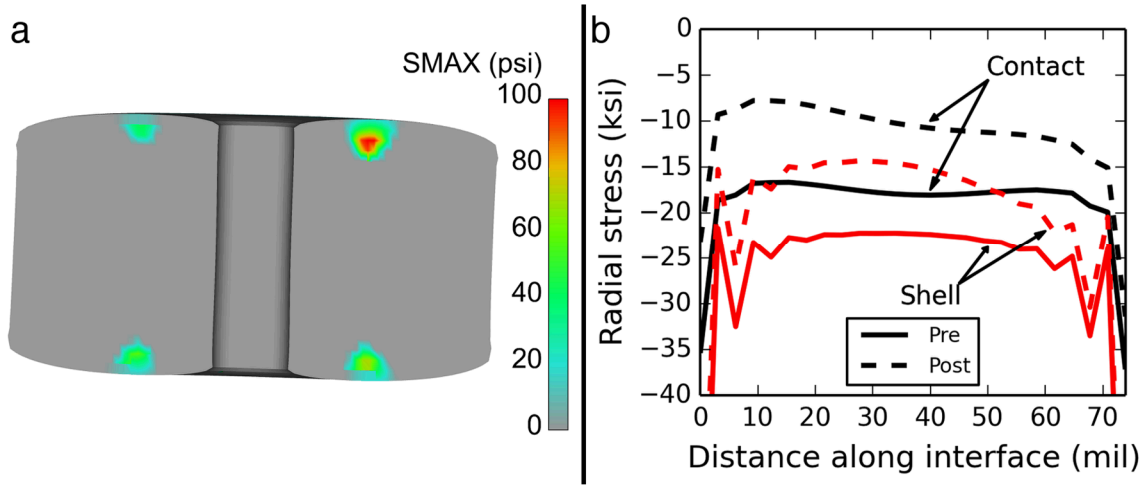

Fig. 9 The post-weld (a) residual maximum principal stress (SMAX) in the glass sealing cycle and (b) pre and post-weld compression at both the shell-glass and contact-glass interface

4 Conclusion

An experimental and numerical analysis of the temperature and residual stress in a hermetic glass-to-metal connector due to laser welding has been conducted. The hermetic connector was welded to a test plate at nominally 350 W and the temperature in the hermetic shell and test plate was measured. It was found that at 350 W, the weld transitioned between keyhole and conduction mode welding. The connector was welded a second time, resulting in a consistent keyhole mode weld. The temperature at the exterior of the shell measured as high as 200 °C. A laser weld modeling technique has been described that allows for modeling the laser welding process and evaluating the temperature and stress in a hermetic connector. The temperature of the glass reached as high as 80 °C during welding. It was shown that there was little change in the residual stress of the sealing glass before and after the laser welding process. The radial compression in the sealing glass was decreased by as much as 10 ksi due to laser welding.

5 References

[1] Glenair Inc., Introduction to Glenair Hermetic Connector Products, www.glenair.com, 2013

[2] Frewin, M.R., Scott, D.A., Finite element model of pulsed laser welding, Welding Research Supplement, 15-22, 1999

[3] De, A., Maiti S.K., Walsh, C.A., Bhadeshia, H.K.D.H., Finite element simulation of laser spot welding, Science and Technology of Welding and Joining, 8(5), 377-384, 2003

[4] Mackwood, A.P., Crafer, R.C., Thermal modelling of laser welding and related processes: a literature review, Optics and Laser Technology, 37, 99-115, 2005

[5] Yilbas, B.S., Arif, A.F.M., Abdul Aleem, B.J., Laser welding of low carbon steel and thermal stress analysis, Optics and Laser Technology, 42, 760-768, 2010

[6] Rońda, J., Siwek, A., Modelling of laser welding process in the phase of keyhole formation, Archives of Civil and Mechanical Engineering, 3, 739-752, 2011

[7] Martinson, P., Daneshpour, S., Koçak, M., Riekehr, S., Staron, P., Residual stress analysis of laser spot welding of steel sheets, Materials and Design, 30, 3351-3359, 2009

[8] Kong, F., Radovan, K., 3D finite element modeling of the thermally induced residual stress in the hybrid laser/arc welding of lap joint, Journal of Materials Processing Technology, 210, 941-950, 2010

[9] Zain-ul-abdein, M., Nélias, D., Jullien, J.F., Deloison, D., Experimental investigation and finite element simulation of laser beam welding induced residual stresses and distortions in thin sheets of AA 6056-T4, Material Science and Engineering A, 527, 3025-3039, 2010

[10] Notz, P.K., Subia, S.R., Hopkins, M.M., Moffat, H.K., Noble, D.R., ARIA Manual Aria 1.5: User's Manual, Sandia National Laboratories, SAND2007-2734, 2007

[11] SIERRA Solid Mechanics Team, Sierra/Solid Mechanics 4.22 User Guide, Sandia National Laboratories, SAND2011-7597, 2011